Canadian Mineralogist
Vol. 29, pp. 255-270 (1991)

PUMPELLYITE AND RELATED MINERALS FROM HYDROTHERMALLY ALTERED ROCKS AT THE KAMIKITA AREA, NORTHERN HONSHU, JAPAN

ATSUYUKI INOUE
Geological Institute, College of Arts and Sciences, Chiba University, Chiba 260, Japan

MINORU UTADA
The University Museum, The University of Tokyo, Tokyo 113, Japan

ABSTRACT

An extensive zone of hydrothermal alteration, characterized by an abundance of CaAl-silicates, is distributed in the Kamikita area, northern Honshu, Japan. This zone is divided into the laumontite and wairakite subzones based upon the distribution of secondary minerals. Pumpellyite-bearing rocks are widespread in the laumontite subzone, whereas hedenbergite- and garnet-bearing rocks are found in the wairakite subzone. Other minerals include prehnite, epidote, chlorite, white mica, albite, titanite, and calcite in both subzones. Textural descriptions and compositional data are presented for the minerals. The estimated temperature of formation of these minerals ranges from 200° to 300°C, as deduced from comparison of the mineral parageneses in the Kamikita area with those in low-grade metamorphism and active geothermal alteration. Fugacities of CO_2 and O_2 range from 1 to 10^{-2} bars and from 10^{-34} to 10^{-47} bars, respectively, assuming that total pressure was controlled by the liquid–vapor equilibrium for H_2O at the temperatures of interest. The $f(CO_2)$ values at Kamikita are lower than those reported from many active geothermal fields, though the $f(O_2)$ values are nearly equivalent. The local decrease in $f(CO_2)$ during the hydrothermal alteration at Kamikita facilitated the formation of pumpellyite and related minerals, which are rare in active geothermal fields.

Keywords: pumpellyite, propylitic alteration, carbon dioxide fugacity, oxygen fugacity, fossil geothermal system, Kamikita, Honshu, Japan.

SOMMAIRE

Le district de Kamikita, dans le nord de l'île de Honshu, au Japon, est le site d'une vaste zone d'altération hydrothermale, dans laquelle les silicates riches en Ca–Al sont répandus. Les sous-zones à laumontite et à wairakite sont définies selon l'abondance des minéraux secondaires. Les roches à pumpellyite sont courantes dans la zone à laumontite, tandis que les roches à hédenbergite et à grenat se limitent à la zone à wairakite. Prehnite, épidote, chlorite, mica blanc, albite, titanite et calcite sont présents dans les deux sous-zones. Nous présentons des descriptions texturales et des données sur la composition de ces minéraux. Leur formation se situerait entre 200 et 300°C, d'après une comparaison des paragenèses avec celles qui caractérisent les ceintures de faible métamorphisme et les zones d'altération hydrothermale. Les fugacités de CO_2 et de O_2 ont varié entre 1 et 10^{-2} bars et entre 10^{-34} et 10^{-47} bars, respectivement, en supposant un contrôle de la pression totale par l'équilibre liquide–vapeur de l'eau aux températures ambiantes. Les valeurs de $f(CO_2)$ à Kamikita sont inférieures à celles de plusieurs champs géothermiques, quoique les intervalles en $f(O_2)$ se ressemblent. La diminution locale en $f(CO_2)$ au cours de l'altération hydrothermale à Kamikita a facilité la formation de la pumpellyite et les minéraux associés, qui sont rares dans les champs géothermiques.

(Traduit par la Rédaction)

Mots-clés: pumpellyite, altération propylitique, fugacité de CO_2, fugacité d'oxygène, système géothermique fossile, Kamikita, île de Honshu, Japon.

INTRODUCTION

The geological significance of pumpellyite has increased since the first description of the mineral by de Roever (1947): it is one of the index minerals for the prehnite–pumpellyite facies of low-grade metamorphism (Coombs 1960). Pumpellyite also occurs in hydrothermally altered oceanic basalts and ophiolites (Coleman 1977, Liou *et al.* 1987), though only a few occurrences of pumpellyite have been documented in rocks collected from mid-oceanic ridges (Sigvaldason 1963, Mével 1981, Viereck *et al.* 1982). Documented occurrences of pumpellyite are even rarer in active geothermal fields, where almost the same temperature conditions as those of low-grade metamorphism prevail. Thus pumpellyite has been considered to be stable under relative higher-pressure conditions. However, pumpellyite generally displays extensive solid-solution, mainly through Fe-for-Al substitution (Coombs *et al.* 1976, Schiffman & Liou 1980, 1983). This variability suggests that the stability of pumpellyite solid solution depends not only on temperature, pressure, and rock composition, but also on the fugacities of oxygen and carbon dioxide, and on fluid composition.

Recently we found two pumpellyite-bearing samples from an area of hydrothermal alteration near the Kamikita Kuroko ore deposit, northern Honshu,

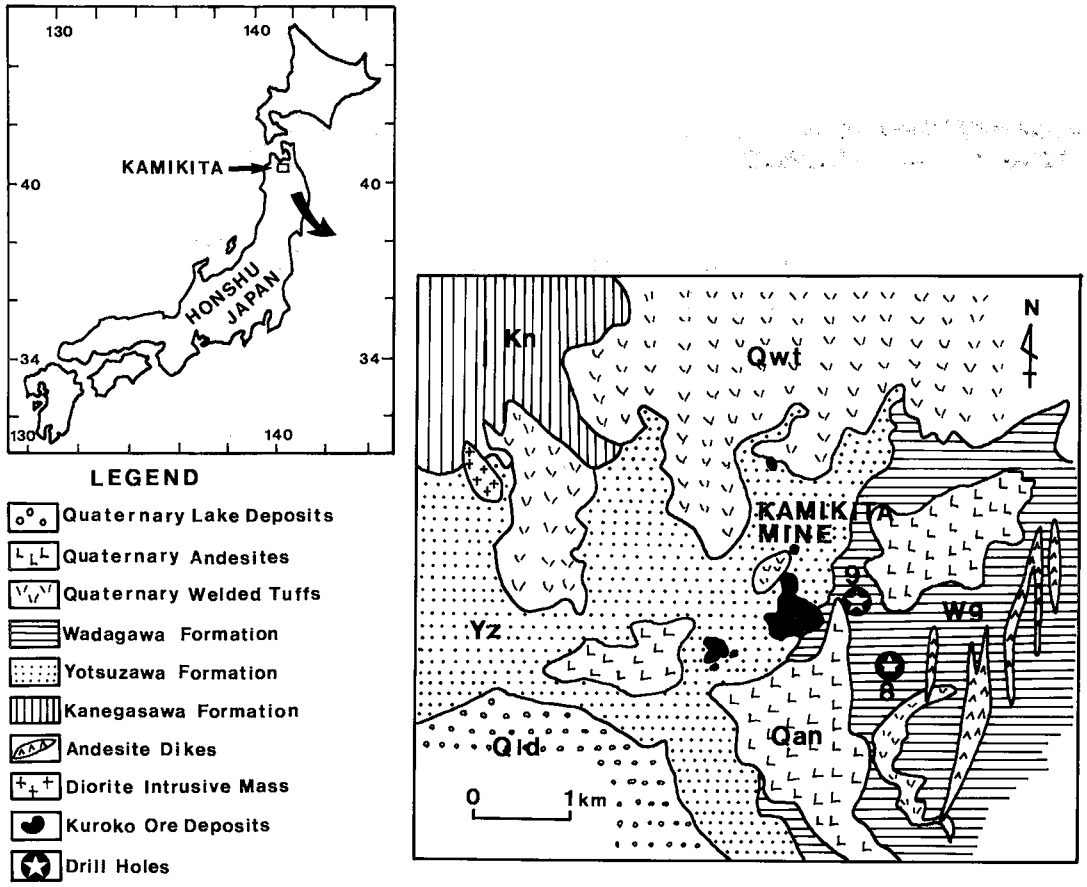

FIG. 1. Geological map of Kamikita area, indicating locations of drill holes used in this study.

Japan. In this paper we describe the mineralogy of pumpellyite and related minerals of hydrothermal origin. We also attempt to estimate the ranges of temperature and fugacities of CO_2 and O_2 during the formation of these minerals.

GEOLOGICAL SETTING

The location and a simplified geological map are shown in Figure 1. In the Kamikita area, marine sediments and volcanic rocks of Miocene to Quaternary age are widely distributed (Miyazima & Mizumoto 1965, 1968, Lee 1970, Lee *et al.* 1974). Rocks of Miocene age constitute the Kanegasawa, Yotsuzawa, and Wadagawa formations, in ascending order. The Kanegasawa Formation is composed of massive or brecciated basaltic to andesitic lava flows. The Yotsuzawa and Wadagawa formations are composed mainly of andesitic to dacitic lava flows and volcaniclastic materials; these rocks are intercalated with layers of mudstones. These Miocene formations dip monoclinally 20°E. They are intruded by small masses of diorite and by andesite dikes. The Quaternary group is divided into three formations, the Tashirodai welded tuffs, andesite lava flows and lake deposits. They unconformably overlie the Miocene sediments.

The two drill holes (Nos. 8 and 9) studied here are located at about 1 km east of the Kamikita Kuroko ore deposit (Fig. 1). They were drilled through the Wadagawa and the Yotsuzawa formations. The former formation contains a thick mudstone at the bottom, and the Kuroko deposits are embedded just below the mudstone.

PETROGRAPHY AND MINERAL ASSEMBLAGES

Figure 2 shows the lithology and the distribution in the drill holes of secondary minerals, which were determined by X-ray powder diffraction and optical microscopy. The mineral assemblage in the mudstones is quite homogeneous and consists of white mica, chlorite, calcite, and quartz. The mudstones occasionally contain late-stage veins of stilbite. On

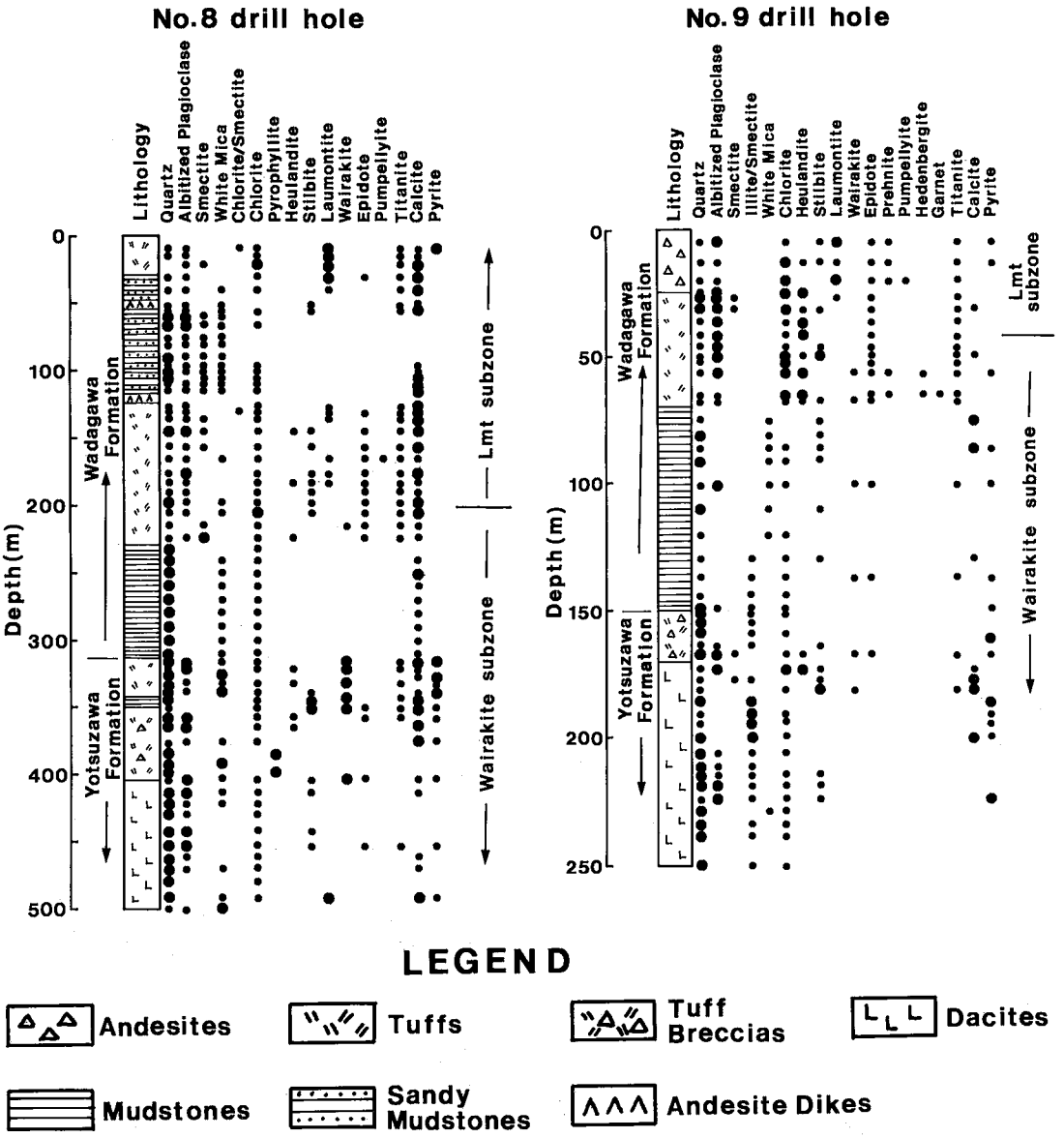

FIG. 2. Lithology and distribution of secondary minerals in the Nos. 8 and 9 drill holes. Abundance of the minerals at various depths is indicated by solid circles; ●: major constituent. •: minor constituent.

the other hand, the mineral assemblages in sandstones and volcanic rocks are variable. The occurrence of pumpellyite, prehnite, hedenbergite, garnet, laumontite, and wairakite is visible in these rocks. The distribution of the secondary minerals shows that the extensive zone of hydrothermal alteration at Kamikita consists of the laumontite and wairakite subzones (Fig. 2). Pumpellyite occurs in the laumontite subzone, and hedenbergite and garnet occur in the wairakite subzone. Prehnite is found in both subzones. These characteristic minerals occur as replacements of feldspar grains, druse fillings, pore fillings, and veins (Fig. 3). Table 1 lists the diagnostic coexisting mineral assemblages observed in druses, interstitial pores, or as pseudomorphs after plagioclase.

The pumpellyite-bearing rocks at Kamikita are characterized by the assemblages pumpellyite + epidote + laumontite + white mica + calcite or pumpellyite + prehnite + epidote + laumontite, determined by optical

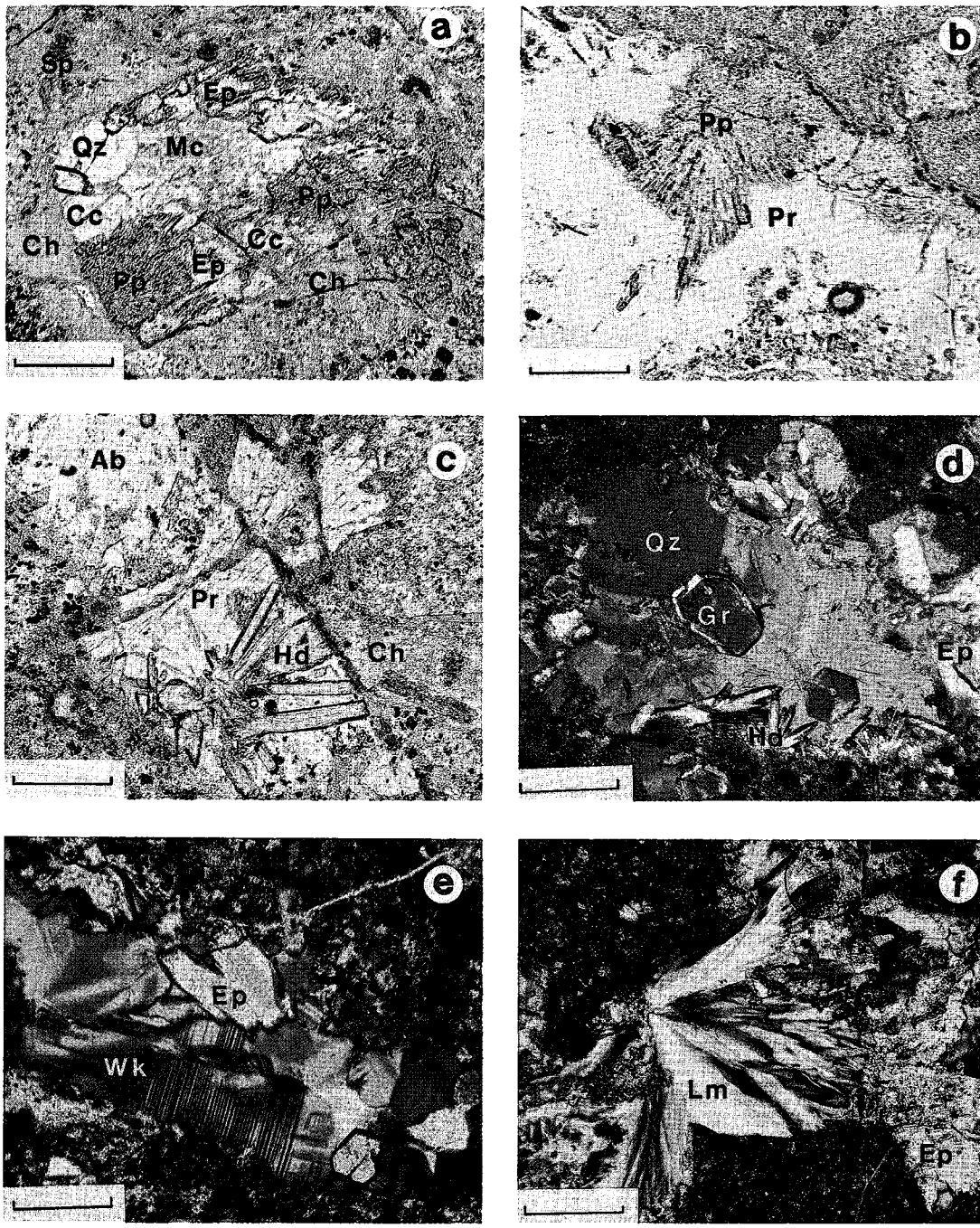

FIG. 3. a) Pumpellyite (Pp) replacing plagioclase phenocryst associated with epidote (Ep), white mica (Mc), quartz (Qz), and calcite (Cc) in sample 8–167 m. b) Radiating acicular aggregates of pumpellyite (Pp) coexisting with prehnite (Pr) in a druse in sample 9–20 m. c) Associated hedenbergite (Hd) and prehnite (Pr) replacing a feldspar grain in sample 9–64 m. The remaining feldspar is albitized (Ab). d) Hedenbergite (Hd), garnet (Gr), and epidote (Ep) filling an interstitial pore space in sample 9–64 m, associated with quartz (Qz). e) Veinlet of wairakite (Wk) associated with epidote (Ep) in sample 9–167 m. f) Laumontite (Lm) associated with epidote (Ep) in sample 920 m. Bars indicate 0.2 mm. Ch: chlorite. Sp: titanite.

microscopy and X-ray-diffraction analysis. The hedenbergite-bearing rocks are characterized by the assemblage hedenbergite + garnet + prehnite + epidote + wairakite. All the assemblages contain chlorite, albite, titanite, and quartz. As shown in Table 1, all the secondary minerals rarely coexist in a single specimen or a single druse. In this study, nevertheless, it is assumed that each assemblage observed within a druse or as a pseudomorphic replacement of feldspar in a thin section has attained local equilibrium.

We note that calcite is abundant through the entire zone of hydrothermal alteration at Kamikita (Fig. 2), but it is commonly rare in the pumpellyite-prehnite-, hedenbergite-, and garnet-bearing rocks except for the pumpellyite-bearing sample from 8–167 m. Heulandite and stilbite are common in sandstones and volcanic rocks of both drill holes (X-ray-diffraction analysis). They occur in late-stage veins or form the final precipitates in druses. The occurrence of pyrite is confined to the lower parts of both drill holes. Pyrophyllite, present over the range of 380–400 m in hole No. 8, may be a product of alteration caused by later acidic hydrothermal activity (Inoue & Utada 1989).

TABLE 1. COEXISTING MINERAL ASSEMBLAGES OBSERVED WITHIN A DRUSE OR AS A REPLACEMENT OF FELDSPAR IN A SINGLE THIN SECTION OF THE KAMIKITA HYDROTHERMALLY ALTERED ROCKS

Calcite-free assemblages		Calcite-bearing assemblages	
Lmt	(9-13 m)		
Wk	(9-56 m, 9-137 m)		
Ep	(9-5 m, 9-13 m, 9-20 m, 9-26 m)		
Ep + Lmt	(9-49 m, 9-56 m)	Ep + Wk + Cal	(8-349 m)
Prh	(9-5 m, 9-13 m, 9-20 m)		
Prh + Ep	(9-20 m, 9-56 m)		
Prh + Ep + Lmt	(9-13 m)		
Pmp + Ep	(9-20 m)	Pmp + Ep + Ms + Cal	(8-167 m)
Pmp + Prh	(9-20 m)		
Pmp + Prh + Ep	(9-20 m)		
Hd + Ep	(9-56 m, 9-64 m)		
Hd + Ep + Lmt	(9-56 m)		
Hd + Ep + Prh	(9-64 m)		
Hd + Ep + Grt	(9-64 m)		

All the assemblages coexist with chlorite, albite, and quartz.
The sample in which the above assemblages were observed is represented in the parentheses. Lmt: laumontite, Wk: wairakite, Ep: epidote, Prh: prehnite, Pmp: pumpellyite, Hd: hedenbergite, Grt: garnet, Ms: white mica, Cal: calcite.

Mineral Chemistry

Pumpellyite

Compositions of pumpellyite are listed in Table

TABLE 2. ELECTRON-MICROPROBE DATA FOR PUMPELLYITE AND PREHNITE IN THE KAMIKITA AREA

	Pumpellyite		Prehnite			
Sample	8-167 m	9-20 m	9-5 m	9-20 m	9-56 m	9-64 m
Number of analyses in average	8	12	2	4	18	11
SiO_2 wt.%	35.9	35.8	42.3	42.4	42.4	41.8
TiO_2	0.02	0.04	-	-	-	-
Al_2O_3	22.2	21.0	20.7	22.1	22.7	20.9
Fe_2O_3	8.33	9.62	4.43	2.93	2.28	5.15
MnO	0.02	0.07	-	-	-	-
MgO	2.66	2.89	0.08	-	0.79	0.36
CaO	22.8	22.6	25.9	26.0	26.2	26.0
K_2O	-	-	-	-	-	0.04
Total	91.93	92.02	93.41	93.43	94.37	94.25
Number of oxygen atoms	24.5	24.5	11	11	11	11
Si	5.91(5.85-5.96)	5.92(5.82-6.00)	3.02(3.01-3.03)	3.01(2.99-3.02)	2.98(2.93-3.01)	2.97(2.95-3.00)
Ti	0.00	0.01	-	-	-	-
Al	4.30(4.00-4.57)	4.08(3.80-4.61)	1.74(1.69-1.79)	1.85(1.77-1.95)	1.88(1.82-1.95)	1.75(1.63-1.90)
Fe^{3+}	1.03(0.68-1.44)	1.20(0.73-1.42)	0.24(0.19-0.28)	0.16(0.09-0.21)	0.12(0.07-0.19)	0.27(0.13-0.41)
Mn	0.00	0.01	-	-	-	-
Mg	0.65(0.59-0.73)	0.71(0.58-0.83)	0.01(0.00-0.02)	-	0.08(0.00-0.25)	0.04(0.00-0.15)
Ca	4.02(3.95-4.07)	4.01(3.97-4.05)	1.99(1.98-1.99)	1.98(1.97-1.99)	1.97(1.92-2.04)	1.98(1.92-2.01)
K	-	-	-	-	-	0.00
Total	15.92(15.91-15.94)	15.93(15.87-15.97)	6.99(6.98-7.00)	6.99(6.99-7.00)	7.03(6.99-7.07)	7.02(7.00-7.04)
X_{Fe}	0.19(0.13-0.27)	0.23(0.14-0.27)	0.24(0.19-0.29)	0.16(0.08-0.21)	0.12(0.07-0.18)	0.27(0.13-0.41)

The values in parentheses indicate the range of analyses. The analyses were determined using an accelerating voltage of 20 kV, a beam current of 200 pA, a beam diameter of 2 μm, and a counting time of 200 s. EDS data were reduced by a ZAF correction scheme. The standard included quartz (Si), corundum (Al), periclase (Mg), metals (Fe, Ti, and Mn), calcite (Ca), albite (Na), and potassium chromate crystal (K).

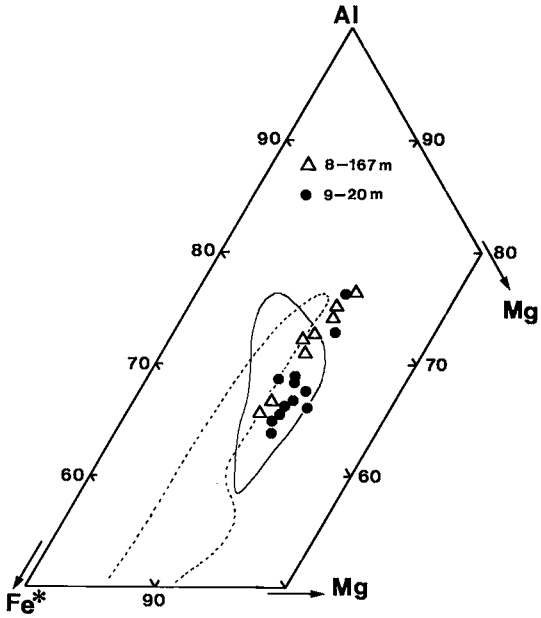

FIG. 4. Compositions of the pumpellyite plotted in Al–Fe*–Mg diagram, expressed as the atomic proportions. Fe* = total Fe. Areas surrounded by solid and dotted lines indicate the compositional fields of pumpellyite from the epidote and zeolite zones, respectively, in the Del Puerto ophiolite, as reported by Evarts & Schiffman (1983).

2. The empirical formula was calculated on the basis of 24.5 oxygen atoms (Nakajima *et al.* 1977), and all the iron (Fe*) was calculated as Fe^{3+}. The Si, Ca, and Mg contents range from 5.82 to 6.00, from 3.95 to 4.07, and from 0.58 to 0.83, respectively. The Ti and Mn contents are negligible. Although green and brown pumpellyites were apparently identified at Kamikita under the microscope, the compositional ranges are essentially identical.

The pumpellyite exhibits a significant range of solid solution by Fe-for-Al substitution. The Fe*/(Fe* + Al) ratio varies from 0.13 to 0.27, with a nearly constant Mg fraction of 0.11 (Fig. 4). The range in the Fe*/(Fe* + Al) ratio in the pumpellyite is more similar to that displayed by pumpellyite coexisting with epidote in low-grade metamorphosed volcanic rocks than that in the zeolite–pumpellyite association (Evarts & Schiffman 1983, Cho *et al.* 1986).

Prehnite

Compositions of prehnite are listed in Table 2, and plotted in the Al–Mg–Fe diagram (Fig. 5). The prehnite at Kamikita can be classified into three groups: the first, typical of prehnite in the 9–20 m sample, is characterized by low Fe and Mg contents (termed Al-rich prehnite in this study); the second (9–56 m sample) is a low-Fe and high-Mg variety (termed Mg-rich prehnite), and the third (9–64 m sample) is a low-

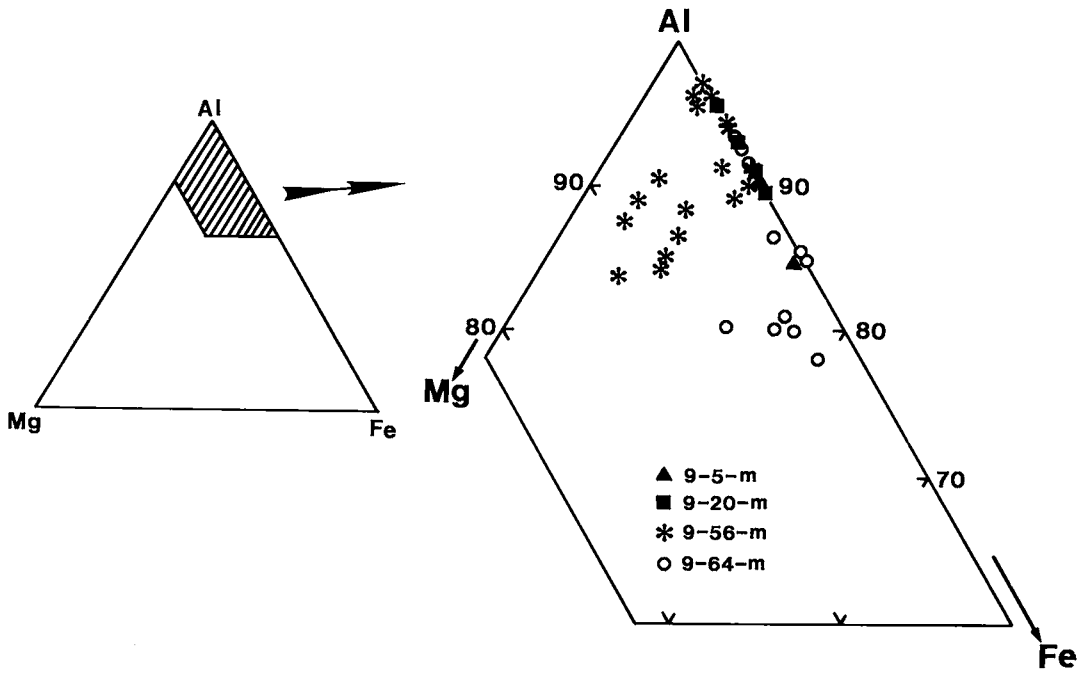

FIG. 5. Compositions of the prehnite plotted in Al–Fe–Mg diagram, expressed in terms of atomic proportions.

TABLE 3. ELECTRON-MICROPROBE DATA FOR EPIDOTE IN THE KAMIKITA AREA

Sample	8-167 m	8-349 m	9-20 m	9-56 m	9-64 m
Number of analyses in average	10	10	13	5	6
SiO_2 wt.%	37.0	37.8	37.0	36.7	36.7
TiO_2	-	-	0.05	-	-
Al_2O_3	24.7	26.0	24.8	22.6	22.4
Fe_2O_3	11.4	10.2	11.2	13.8	14.4
MnO	0.08	0.27	0.19	0.17	0.01
MgO	-	-	0.04	0.03	-
CaO	23.2	23.6	23.1	23.2	23.3
Total	96.38	97.87	96.38	96.50	96.81
Number of oxygen atoms	25	25	25	25	25
Si	5.96(5.94-5.97)	5.93(5.90-5.96)	5.94(5.90-5.97)	5.96(5.93-6.02)	5.95(5.93-5.99)
Ti	-	-	0.01	-	-
Al	4.68(4.37-5.02)	4.84(4.67-5.00)	4.70(4.16-5.09)	4.32(4.06-4.49)	4.28(3.74-4.81)
Fe^{3+}	1.37(1.02-1.66)	1.20(1.07-1.39)	1.35(1.00-1.85)	1.68(1.52-1.89)	1.75(1.26-2.23)
Mn	0.01(0.00-0.03)	0.04(0.01-0.08)	0.02(0.01-0.07)	0.02(0.02-0.03)	0.01(0.00-0.03)
Mg	-	-	0.01	0.01	-
Ca	4.00(3.91-4.04)	3.99(3.91-4.08)	3.99(3.89-4.02)	4.03(4.00-4.08)	4.05(4.03-4.09)
Total	16.02(15.97-16.03)	16.01(15.93-16.06)	16.02(15.99-16.06)	16.03(16.00-16.05)	16.04(16.03-16.06)
X_{Ps}	0.23(0.17-0.28)	0.20(0.18-0.23)	0.22(0.14-0.31)	0.28(0.25-0.32)	0.29(0.21-0.38)

The values in parentheses indicate the range of analyses.

Mg and high-Fe variety (termed Fe-rich prehnite). The Al-rich prehnite contains 8 to 21 mol% of the ferrian prehnite end member $Ca_2FeAlSi_3O_{10}(OH)_2$ and coexists with pumpellyite in andesite lavas. The Mg-rich prehnite has $X_{\text{Fe-prehnite}}$ of 0.07–0.18 and coexists with epidote in sandstones. The $X_{\text{Fe-prehnite}}$ of the Fe-rich prehnite ranges from 0.13 to 0.41. It generally coexists with hedenbergite in sandstones. All the prehnite varieties coexist with chlorite. The 9–5 m sample, which was originally andesite lava, may be said to contain an Al-rich variety, based on the few analyses obtained.

Epidote

Compositions of epidote are listed in Table 3. The epidote at Kamikita contains between 13.7 and 37.4% pistacite $Ca_2Fe_3Si_3O_{12}(OH)$. Each epidote grain shows a slight compositional zoning, but no systematic trend was detected. The X_{Ps} is greater in epidote coexisting with the Mg-rich and Fe-rich prehnites (9–56 m and 9–64 m samples) than those with the Al-rich prehnite and without prehnite. In particular, the X_{Ps} of epidote in the 9–64 m sample attains 0.38. The apparent distribution coefficient, K_d, for Fe–Al partition between epidote and prehnite ranges from 0.025 to 0.09 (Fig. 6), where the composition $Ca_2FeAl_2Si_3O_{12}(OH)$ is considered as one end member of epidote, according to Rose & Bird (1987). The Mn content is negligible.

Chlorite

Compositions of chlorite are listed in Table 4. The chlorite contains between 2.79 and 3.03 Si per $O_{10}(OH)_8$. The ratio Fe/(Fe+Mg) varies from 0.16 to 0.54 (Fig. 7). The relatively Fe-rich compositions coexist with Mg-rich prehnite and Fe-rich epidote (9–56 m sample), and with Fe-rich prehnite, Fe-rich epidote, hedenbergite, and garnet (9–64 m sample). The Fe-rich chlorite in the 8–54 m sample occurs as veins with phengitic mica. The occurrence of chlorite having an intermediate Fe/(Fe+Mg) ratio is diagnostic of the association with pumpellyite or Al-rich prehnite or both (8–167 m and 9–20 m samples). The occurrence of Fe-poor chlorite is confined to the deeper parts of both drill holes, in which it coexists with white mica and illite–smectite. The composition of the Fe-poor chlorite is close to that of chlorite in hydrothermally altered rocks related to Kuroko mineralization (Inoue, unpubl. data).

Hedenbergite

The hedenbergite (Table 5) contains a mole fraction of diopside ($CaMgSi_2O_6$) between 0 and 0.51 (Fig. 8a). In addition, it is characterized by high Mn content (from 0.38 to 3.93 wt.% MnO). The proportion of the johannsenite component is inversely proportional to the Mg content (diopside component), as shown in Figure 8b.

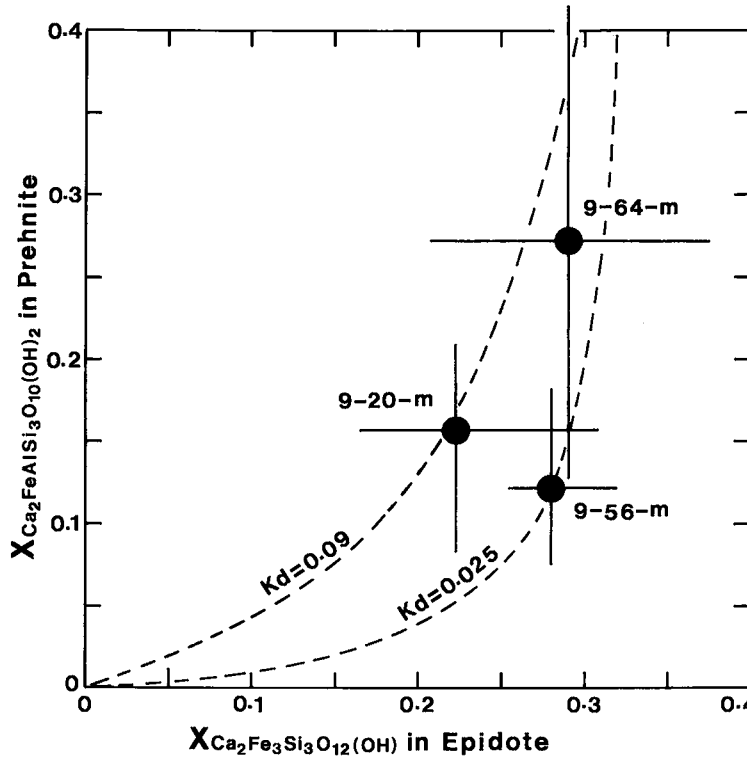

FIG. 6. Distribution of Fe^{3+} between coexisting epidote and prehnite, expressed as the mole fraction of $Ca_2FeAlSi_3O_{10}(OH)_2$ in prehnite and $Ca_2Fe_3Si_3O_{12}(OH)$ (pistacite) in epidote. Solid circles and bars represent average compositions and ranges, respectively. Dashed curves represent values of constant distribution coefficient K_d for the reaction Al-prehnite + epidote = Fe-prehnite + clinozoisite, where the composition $Ca_2FeAl_2Si_3O_{12}(OH)$ was assumed as an end member for epidote.

Garnet

Although the garnet shows a complex solid-solution between pyrope, almandine, spessartine, and grossular, the composition can be essentially represented by almandine–spessartine solid solutions (Table 5). The estimated hydrogrossular content is negligible (less than 2%).

Zeolites

The composition of zeolites is given in Table 6. Laumontite contains a small amount of alkalis replacing calcium. Wairakite is close to the Ca-end member and does not show solid solution with analcime. Stilbite and heulandite have a Al/(Al + Si) ratio of 0.25-0.27 and a $R^+/(R^+ + R^{2+})$ of 0.07-0.32. No systematic change in the compositions of the zeolites was detected in the two drill cores.

Other hydrothermal minerals

Calcite is almost pure in composition. Titanite in the 9–64 m sample shows about 20% of Al-for-Ti substitution. The white mica is usually phengitic, containing about 25 mol % of the celadonite component (Table 7).

FORMATION OF PUMPELLYITE AND RELATED MINERALS IN THE KAMIKITA HYDROTHERMAL SYSTEM

Based upon the parageneses and compositional variations of secondary minerals described above, two diagnostic mineral assemblages, A and B, are identified in the extensive zone of Kamikita hydrothermal alteration. Assemblage A is pumpellyite + Al-rich prehnite + Fe-poor epidote + intermediate Fe-bearing chlorite. Assemblage B con-

TABLE 4. ELECTRON-MICROPROBE DATA FOR CHLORITE IN THE KAMIKITA AREA

Sample	8-54 m	8-167 m	9-5 m	9-20 m	9-56 m	9-64 m	9-167 m
Number of analyses in average	3	5	4	3	4	9	3
SiO_2 wt.%	26.9	27.5	28.0	28.7	24.6	27.8	28.1
Al_2O_3	16.6	17.4	16.8	18.4	17.5	17.5	19.9
FeO	29.0	20.6	22.1	19.1	23.6	24.0	9.8
MnO	-	0.23	0.28	0.34	0.40	0.36	-
MgO	13.8	18.4	18.7	19.8	13.5	15.6	27.1
CaO	-	0.31	0.14	0.34	0.14	0.15	0.02
K_2O	-	0.05	0.05	0.05	0.02	0.01	-
Total	86.3	84.49	86.07	86.73	79.76	85.42	84.92
Number of oxygen atoms	14	14	14	14	14	14	14
Si	2.95(2.94-2.95)	2.94(2.92-2.97)	2.96(2.95-2.97)	2.95(2.93-2.97)	2.86(2.84-2.90)	2.99(2.94-3.03)	2.81(2.79-2.82)
Al	2.14(2.10-2.17)	2.19(2.15-2.23)	2.09(2.07-2.11)	2.23(2.20-2.25)	2.39(2.34-2.45)	2.25(2.09-2.56)	2.35(2.31-2.37)
Fe	2.65(2.62-2.68)	1.84(1.82-1.86)	1.96(1.94-1.98)	1.64(1.60-1.70)	2.29(2.22-2.36)	2.16(2.05-2.24)	0.82(0.80-0.83)
Mn	-	0.02	0.02	0.03	0.04	0.03	-
Mg	2.25(2.23-2.26)	2.93(2.89-2.99)	2.95(2.90-2.98)	3.03(3.01-3.05)	2.35(2.30-2.41)	2.50(2.46-2.57)	4.04(4.01-4.09)
Ca	-	0.03	0.02	0.04	0.02	0.02	0.00
K	-	0.01	0.01	0.01	0.00	0.00	-
Total	9.99(9.98-10.00)	9.97(9.95-9.98)	10.00(9.99-10.01)	9.93(9.92-9.95)	9.94(9.92-9.97)	9.95(9.85-9.99)	10.02(10.01-10.03)
X_{Fe}(= Fe/(Fe+Mg))	0.54	0.39(0.38-0.39)	0.40(0.39-0.41)	0.35(0.35-0.36)	0.49(0.48-0.51)	0.46(0.45-0.47)	0.17(0.16-0.17)

The values in parentheses indicate the range of analyses.

sists of hedenbergite + garnet + Fe-rich prehnite + Fe-rich epidote + Fe-rich chlorite. The assemblages are illustrated schematically in the Al–Mg–(Fe* + Mn) diagram (Fig. 9). Both assemblages contain albite, titanite, and quartz. In addition, laumontite and white mica are included in assemblage A, and wairakite in assemblage B. Although most of the two- and three- phase assemblages denoted in Figure 9 have been observed petrographically or inferred by X-ray-diffraction analysis, as shown in Table 1, the critical low-variance assemblages including pumpellyite and related minerals are distinctly rare. Therefore, the nature of the reactions that define isograds is poorly understood at Kamikita. The assemblages A and B were apparently identified in the laumontite and wairakite subzones, respectively. This suggests that the temperature of formation of assemblage B was probably slightly higher than that for assemblage A, but the difference in mineral assemblages and chemical composition of each mineral may be governed mostly by local difference in bulk composition.

As for the formation of pumpellyite and related minerals, no direct measurements of temperature are available in the Kamikita field. The range of temperature of formation of the above mineral assemblages can be estimated by analogy with information on low-grade metamorphic terranes and active geothermal fields. With respect to assemblage A, Evarts & Schiffman (1983) gave a minimum temperature of 125°C for the appearance of pumpellyite associated with zeolites in the Del Puerto ophiolite. Their pumpellyite contains much more Fe than that in their epidote zone. The Kamikita pumpellyite is closer in Fe*/(Fe* + Al) ratio to that in the epidote zone at Del Puerto, as mentioned in the preceding section. Epidote appears generally at temperatures of 200° to 250°C in geothermal fields (Browne 1978, Henley & Ellis 1983, Bird *et al.* 1984). In the geothermal fields of Iceland, the measured temperature of pumpellyite-bearing rocks ranges from 180 to 230°C (Sigvaldason 1963). Experimentally, the temperature

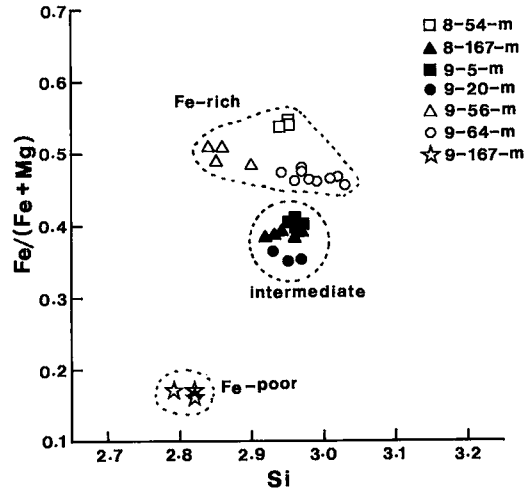

FIG. 7. Compositions of chlorite plotted in terms of Si *versus* Fe/(Fe + Mg) ratio.

TABLE 5. ELECTRON-MICROPROBE DATA FOR HEDENBERGITE AND GARNET IN THE KAMIKITA AREA

	Hedenbergite		Garnet
Sample	9-64 m		9-64 m
Number of analyses in average	19		4
SiO_2 wt.%	50.1		36.4
TiO_2	-		0.14
Al_2O_3	0.82		21.2
FeO	19.8		22.2
MnO	2.15		14.0
MgO	3.68		1.65
CaO	23.2		3.23
Total	99.75		98.82
Number of oxygen atoms	6		12
Si	2.00(1.98-2.02)		2.98(2.97-2.99)
Ti	-		0.01
Al	0.04(0.00-0.11)		2.04(2.02-2.07)
Fe	0.66(0.43-0.85)		1.51(1.40-1.66)
Mn	0.07(0.02-0.14)		0.96(0.84-1.09)
Mg	0.21(0.00-0.47)		0.20(0.17-0.22)
Ca	0.99(0.97-1.01)		0.29(0.25-0.32)
Total	3.98(3.97-4.00)		7.99(7.99-8.00)
X_{Di}	0.22(0.00-0.51)	X_{Prp}	0.07(0.06-0.07)
X_{Hd}	0.70(0.54-0.84)	X_{Alm}	0.51(0.47-0.55)
X_{Jh}	0.07(0.02-0.16)	X_{Sps}	0.32(0.28-0.36)
		X_{Grs}	0.10(0.08-0.11)
		X_{Hgr}	0.01(0.00-0.02)

The values in parentheses indicate the range of analyses. Di: diopside, Hd: hedenbergite, Jh: johannsenite, Prp: pyrope, Alm: almandine, Sps: spessartine, Grs: grossular, Hrs: hydrogrossular.

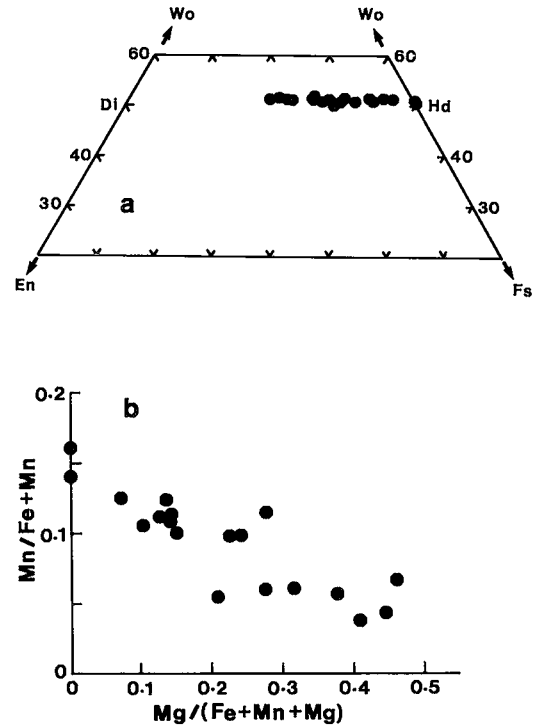

FIG. 8. a) Compositions of hedenbergite in sample 9-64 m plotted in the pyroxene quadrilateral. En: enstatite ($Mg_2Si_2O_6$), Fs: ferrosilite ($Fe_2Si_2O_6$), Di: diopside ($CaMgSi_2O_6$), Hd: hedenbergite ($CaFeSi_2O_6$), Wo: wollastonite ($Ca_2Si_2O_6$). b) Relation of Mn/(Fe+Mn) and Mg/(Fe+Mn+Mg) ratios in hedenbergite from Kamikita.

of the reaction in which the Fe end member of pumpellyite breaks down to epidote + H_2O is considered to be about 200°C at 1 kbar (Liou 1979, Schiffman & Liou 1983). The temperature of the reaction shifts toward lower temperatures with decreasing total pressure, but toward higher temperatures with decreasing Fe content in pumpellyite. Increasing $f(O_2)$ also contributes to a decrease in the thermal stability (Schiffman & Liou 1983). Thus, the minimum temperature of formation of the pumpellyite-bearing assemblage at Kamikita is considered to be about 200°C.

Elders *et al.* (1981) and Cavarretta *et al.* (1982) reported a similar mineral assemblage to assemblage B, *i.e.*, prehnite, hedenbergite, epidote, and actinolite, from the Cerro Prieto and Larderello geothermal fields, respectively. They suggested a range in temperature of formation from 250° to 350°C. Hydrothermal actinolite, clinopyroxene, and garnet appear generally at temperatures greater than 300°C (Browne 1978, Henley & Ellis 1983, Bird *et al.* 1984). Actinolite is absent in the Kamikita area. The hedenbergite and garnet contain a significant proportion of the Mn-component. The stability of the Mn-substituted minerals expands toward lower temperatures compared to the Mn-free equivalents (Hsu 1968). This suggests that the maximum temperature did not exceed 300°C at Kamikita. Consequently, the temperature range of 200° to 300°C is taken as a reasonable value for the formation of pumpellyite and related minerals at Kamikita.

The K_d values (0.025–0.09) that govern the Fe-Al partition between epidote and prehnite in assemblages A and B (Fig. 6) indicate the temperature to be approximately between 150° and 350°C, if we assume the activity–composition relations and thermodynamic properties for epidote and prehnite reported by Bird & Helgeson (1980) and Rose & Bird (1987). The partition of Fe and Al between epidote and prehnite at Kamikita is similar to that at Cerro Prieto, where the two minerals equilibrated at 200°–370°C (Schiffman *et al.* 1985). This suggests that the distribution of octahedrally coordinated cations among the coexisting minerals at Kamikita approached chemical equilibrium on the microscopic level in the temperature range of 200–300°C, estimated above on the basis of mineral parageneses.

TABLE 6. ELECTRON-MICROPROBE DATA FOR STILBITE, HEULANDITE, LAUMONTITE, AND WAIRAKITE IN THE KAMIKITA AREA

	Stilbite			Heulandite	Laumontite	Wairakite	
Sample	8-349 m	9-56 m	9-167 m	9-56 m	9-5 m	8-349 m	9-137 m
Number of analyses in average	6	8	3	4	4	5	3
SiO_2 wt.%	58.3	58.7	56.4	57.7	52.0	53.3	53.1
Al_2O_3	17.8	17.3	16.7	16.7	20.8	23.4	23.3
Fe_2O_3	0.02	-	-	-	0.20	-	-
CaO	8.19	8.10	7.45	7.92	10.3	12.7	12.5
Na_2O	0.79	0.28	0.81	-	0.43	-	-
K_2O	0.23	0.43	0.27	0.56	0.32	0.05	-
Total	85.33	84.81	81.63	82.88	84.05	89.45	88.9
Number of oxygen atoms	72	72	72	72	72	12	12
Si	26.60(26.58-26.76)	26.90(26.48-27.07)	26.84(26.62-27.09)	27.02(26.62-27.26)	24.54(24.48-24.66)	3.96(3.94-3.98)	3.96(3.95-3.98)
Al	9.58(9.45-9.91)	9.32(9.06-9.79)	9.38(9.00-9.64)	9.21(8.92-9.68)	11.58(11.34-11.59)	2.05(2.02-2.06)	2.05(2.03-2.06)
Fe	0.01	-	-	-	0.04	-	-
Ca	4.00(3.71-4.20)	3.98(3.62-4.08)	3.80(3.60-4.06)	3.97(3.91-4.06)	5.22(5.11-5.23)	1.01(1.00-1.02)	1.00(0.99-1.01)
Na	0.70(0.40-1.37)	0.25(0.00-1.08)	0.75(0.35-1.26)	-	0.42(0.32-0.60)	-	-
K	0.13(0.01-0.35)	0.25(0.03-0.43)	0.16(0.13-0.21)	0.33(0.29-0.41)	0.18(0.16-0.24)	0.00	-
Total	41.02(40.83-41.63)	40.69(40.54-40.99)	40.93(40.66-41.25)	40.54(40.43-40.70)	41.98(41.80-42.18)	7.02(7.01-7.03)	7.01(7.00-7.02)
Al/(Al+Si)	0.27(0.26-0.27)	0.26(0.25-0.27)	0.26(0.25-0.27)	0.25(0.25-0.27)	0.32		
$R^+/(R^+ + R^{2+})$	0.17(0.11-0.32)	0.11(0.08-0.24)	0.19(0.11-0.28)	0.08(0.07-0.09)	0.10(0.10-0.17)		

The values in parentheses indicate the range of analyses.

TABLE 7. ELECTRON-MICROPROBE DATA FOR WHITE MICA, TITANITE, AND CALCITE IN THE KAMIKITA AREA

	White mica				Titanite		Calcite
Sample	8-54 m	8-167 m	9-137 m		9-64 m		8-167 m
Number of analyses in average	7	1	1		1		1
SiO_2 wt.%	49.0	49.2	47.6	SiO_2 wt.%	30.6	FeO wt.%	0.27
TiO_2	0.11	-	0.38	TiO_2	30.7	MnO	0.11
Al_2O_3	29.2	32.3	34.1	Al_2O_3	5.06	MgO	0.20
FeO	2.80	1.30	0.63	CaO	28.5	CaO	54.2
MgO	2.58	2.13	2.77	Total	94.86	Sum	54.78
CaO	0.76	0.48	0.16	Number of oxygen atoms	5	Eq. CO_2	44.01
Na_2O	0.17	0.37	0.56			Total	98.79
K_2O	8.31	9.81	10.7	Si	1.04	Fe	0.004
Total	92.93	95.59	96.90	Ti	0.79	Mn	0.002
Number of oxygen atoms	11	11	11	Al	0.20	Mg	0.005
				Ca	1.04	Ca	0.99
Si	3.32(3.29-3.35)	3.24	3.11	Total	3.07		
Al	2.33(2.29-2.42)	2.51	2.63				
Ti	0.01	-	0.02				
Fe	0.16(0.15-0.17)	0.07	0.03				
Mg	0.26(0.17-0.30)	0.21	0.27				
Ca	0.06(0.04-0.07)	0.03	0.01				
Na	0.02(0.00-0.06)	0.05	0.07				
K	0.72(0.66-0.79)	0.82	0.89				
a(Muscovite)*	0.6	0.6	0.6				

The values in parentheses indicate the range of analyses.
* The activity of muscovite component in white mica was calculated using the activity-composition relation reported by Helgeson et al. (1978).

The detailed distribution of octahedrally coordinated cations among coexisting minerals at Kamikita has not as yet been investigated.

Fugacities of CO_2 and O_2 also influenced the formation of pumpellyite and related minerals. They were estimated assuming liquid–vapor equilibrium for H_2O at the temperatures of interest. Equations and thermodynamic data required in the calculations were adopted from the internally consistent data-set given by Helgeson and his colleagues (Helgeson &

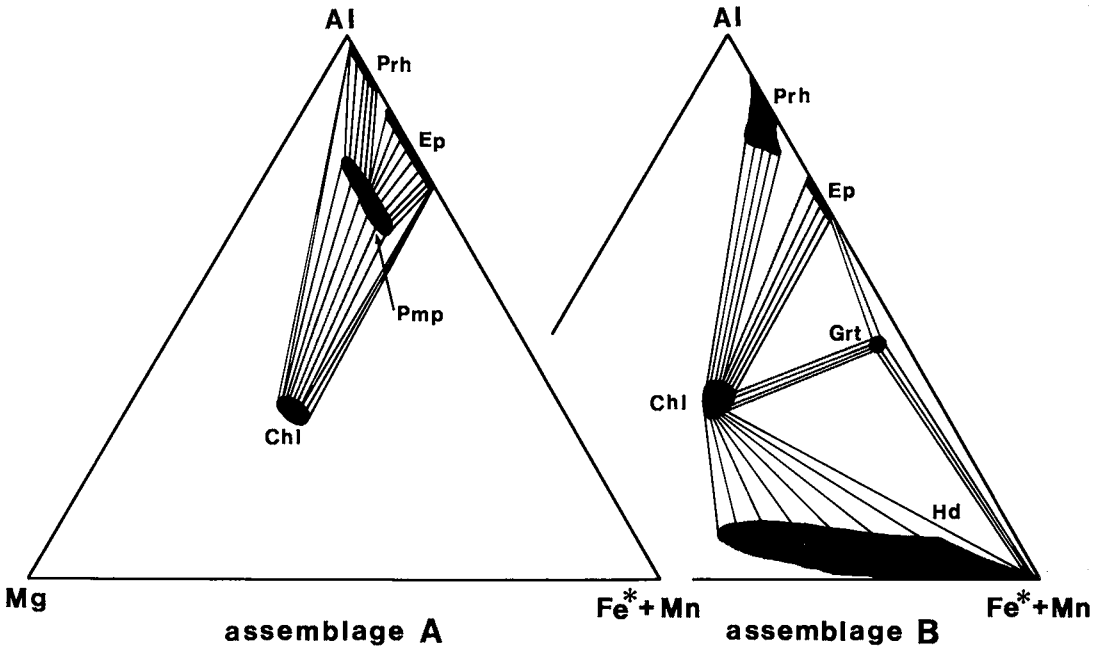

FIG. 9. Two diagnostic mineral assemblages in the extensive zone of Kamikita hydrothermal alteration, illustrated in terms of Al–Mg–(Fe* + Mn). Chl: chlorite, Pmp: pumpellyite, Prh: prehnite, Ep: epidote, Grt: garnet, Hd: hedenbergite.

Kirkham 1974, Helgeson *et al.* 1978, Helgeson *et al.* 1981). Nonstoichiometry in epidote, prehnite, hedenbergite, and white mica is accounted for by activity–composition relations for thermodynamic components of solid solutions reported by Helgeson *et al.* (1978), Bird & Helgeson (1980), and Rose & Bird (1987).

Figure 10 shows the T – log $f(CO_2)$ relationships in the system $CaO–Al_2O_3–SiO_2–H_2O–CO_2$, where calcite has equilibrated with the silicates. If $a(SiO_2)$ is fixed by saturation with quartz and $a(H_2O)$ is equal to 1, margarite appears stably instead of wairakite above 230°C in the T – log $f(CO_2)$ diagram. Wairakite is stable only under conditions of higher $a(SiO_2)$. In fact, however, wairakite occurs commonly with quartz, and no margarite was identified at Kamikita. This inconsistency may be a result of the uncertainty of the thermodynamic data-set used.

Since there are no reliable thermodynamic data for pumpellyite, $f(CO_2)$ cannot be estimated directly from the equilibrium reaction concerning the formation of pumpellyite. In spite of that, the range of log $f(CO_2)$ at Kamikita can be estimated by assuming the following equilibrium reactions among the coexisting mineral assemblages in the pumpellyite-bearing rocks, as shown in Table 1:

3 white mica + 4 calcite + 6 quartz =
2 clinozoisite + 3 K-feldspar + $4CO_2$ + $2H_2O$ (1)

and

2 clinozoisite + 3 quartz + 2 calcite + $2H_2O$ =
3 prehnite + $2CO_2$ (2)

Equations (1) and (2) were calculated using the compositional data for epidote and white mica in the 8–167 m sample and for epidote and prehnite in the 9–20 m, 9–56 m, and 9–64 m samples, respectively. Then, it was assumed that a(muscovite) was 0.6 (Table 7), and that a(quartz), a(calcite), and $a(H_2O)$ were equal to 1. The presence of K-feldspar has not yet been defined in the 8–167 m sample. Nevertheless, we assumed the presence of K-feldspar in the sample, and a value of a(K-feldspar) equal to 1 for the sake of the thermodymanic calculations. The Kamikita samples are actually calcite-free except for the 8–167 m sample. The log $f(CO_2)$ equilibrated with the Kamikita epidote and prehnite solid solutions was lower than the calculated curves in Figure 10. The $f(CO_2)$ ranged from 1 to 10^{-2} bar, as shown by the shadowed area in Figure 10. The $f(CO_2)$ values at Kamikita are lower than those in many geothermal fields, *e.g.*, $10^{0.5}$–10^{1} bars at Salton Sea (Bird & Helgeson 1981), about 1 bar at Larderello (Cavarretta *et al.* 1982), and $10^{-0.5}$–$10^{0.5}$ bars in the New Zealand geothermal fields (Giggenbach 1980, 1981).

The range of $f(O_2)$ at Kamikita can be estimated by the equilibrium assemblage of hedenbergite, epi-

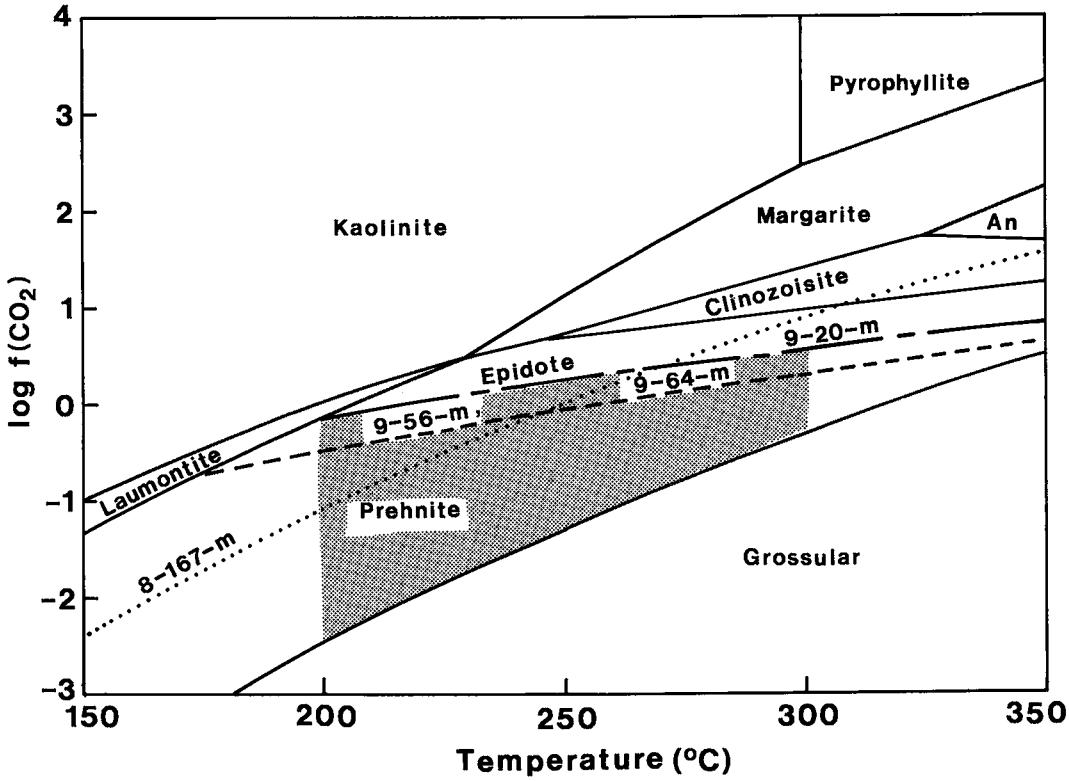

FIG. 10. Range in fugacity of carbon dioxide $f(CO_2)$ and temperature for the formation of pumpellyite and related minerals at Kamikita. Phase relations in the system $CaO–Al_2O_3–SiO_2–H_2O–CO_2$ were calculated using the data given by Helgeson *et al.* (1978) and on the assumption that quartz and calcite are in equilibrium with the silicates. The two dashed curves represent the locus of prehnite – epidote coexistence in samples 9–20 m, 9–56 m, and 9–64 m, calculated for the reaction (2) in the text. The dotted curve represents the locus of epidote – white mica coexistence in sample 8–167 m, calculated according to reaction (1) in the text. An: anorthite.

dote, and prehnite present in the 9–64 m sample. The variation of $\log f(O_2)$ with temperature is shown in Figure 11. The estimated $f(O_2)$ at Kamikita ranged from 10^{-47} to 10^{-34} bars. This range is close to that estimated for many geothermal fields (D'Amore & Panichi 1980, D'Amore & Gianelli 1984).

In summary, the hydrothermal alteration that formed pumpellyite and related minerals at Kamikita took place between 200° and 300°C, at a $f(CO_2)$ between 1 and 10^{-2} bars, at a $f(O_2)$ of 10^{-34} – 10^{-47} bars, and at a P(total) of less than 1 kbar (the pressure was probably controlled by liquid–vapor equilibrium for H_2O at those temperatures). These conditions are quite normal in most geothermal fields, except for $f(CO_2)$, which is significantly lower at Kamikita. A.L. Albee and E-An Zen [cited by Bishop (1972)] and Seki (1973) emphasized the critical role of CO_2 in determining the stability of pumpellyite and prehnite in low-grade metamorphic assemblages under conditions of constant temperature and total pressure. As demonstrated in the Kamikita area, the pumpellyite + prehnite assemblage can have formed even in an environment of low total pressure if $f(CO_2)$ was locally low. Where $f(CO_2)$ increased, the pumpellyite and prehnite would be replaced by the assemblages epidote + chlorite + calcite, and finally chlorite + calcite under conditions of nearly constant temperature and total pressure. The chemical potential of CO_2 may be generally high in geothermal fields compared to regional metamorphic terranes. Propylitic alteration, characterized by the assemblage epidote + chlorite + calcite without pumpellyite or prehnite, thus occurs more commonly in geothermal fields.

ACKNOWLEDGEMENTS

We are indebted to Dr. H. Tatematsu, Japan Railway Research Institute, for the core samples used in this study. Thanks are also extended to Drs. R.F. Martin, G.K. Czamanske, and S.D. McDowell and an anonymous referee for critical review of the

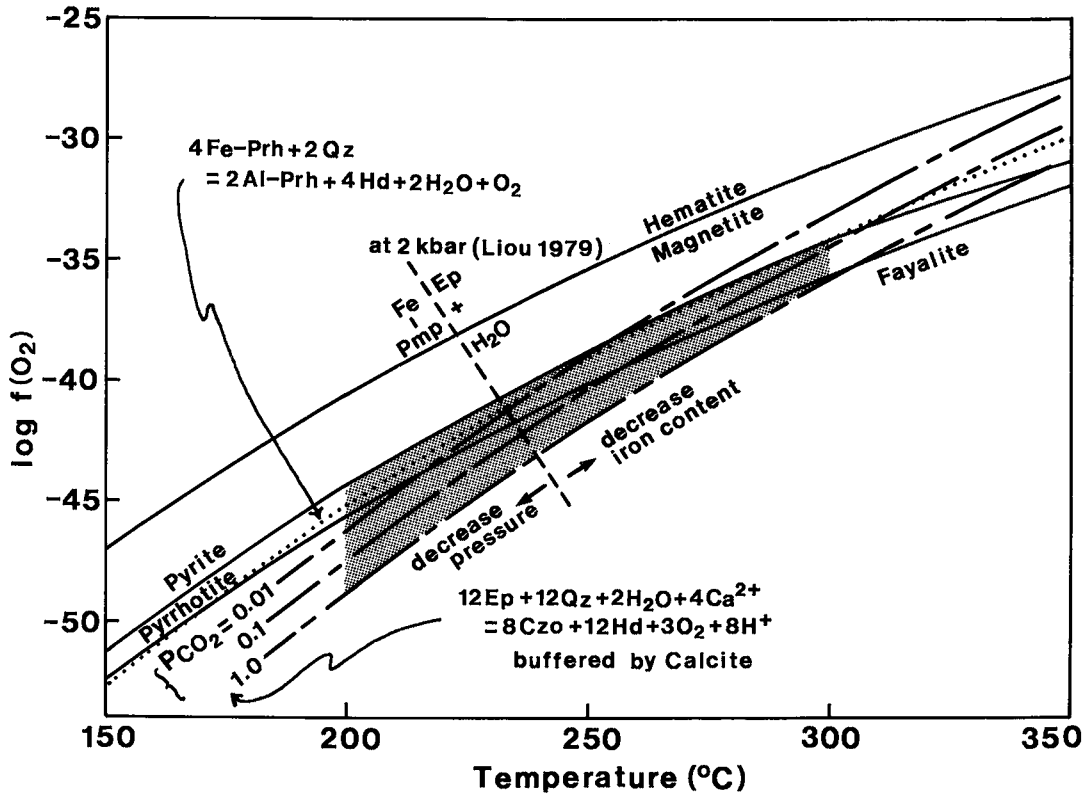

FIG. 11. Range in fugacity of oxygen $f(O_2)$ and temperature for the formation of pumpellyite and related minerals at Kamikita. The three dashed curves represent the locus of epidote – hedenbergite coexistence at constant CO_2 partial pressure, 0.01, 0.1, and 1.0 bar, in sample 9–64 m. The curves were calculated for the reaction, 12 epidote + 12 quartz + $2H_2O$ + $4Ca^{2+}$ = 8 clinozoisite + 12 hedenbergite + $3O_2$ + $8H^+$, assuming that Ca^{2+}/H^+ ratio is buffered by calcite. Dotted curve represents the locus of prehnite – hedenbergite coexistence in sample 9–64 m, calculated for the reaction, 4 Fe-prehnite + 2 quartz = 2 Al-prehnite + 4 hedenbergite + $2H_2O$ + O_2, where the compositions $Ca_2FeAlSi_3O_{10}(OH)_2$ and $Ca_2Al_2Si_3O_{10}(OH)_2$ were assumed for the Fe- and Al-prehnite, respectively. The transversal dashed line represents the approximate $f(O_2)$-T limit at 2 kbars for the reaction, 2 Fe-pumpellyite $[Ca_4Fe^{2+}\ Fe^{3+}Al_4Si_6O_{21}(OH)_7]$ + $0.5O_2$ = 4 epidote + $5H_2O$, cited from Liou (1979). Solid curves represent $f(O_2)$ values defined by the hematite-magnetite, fayalite-magnetite-quartz, and pyrite–pyrrhotite buffers.

manuscript. This study was financed in part by a Grant-in-Aid for Scientific Research of the Ministry of Education of Japan (No. 02640621/A.I).

REFERENCES

BIRD, D.K. & HELGESON, H.C. (1980): Chemical interaction of aqueous solutions with epidote–feldspar mineral assemblages in geologic systems. I. Thermodynamic analysis of phase relations in the system CaO–FeO–Fe_2O_3–Al_2O_3–SiO_2–H_2O–CO_2. *Am. J. Sci.* **280**, 907-941.

_____ & _____ (1981): Chemical interaction of aqueous solutions with epidote–feldspar mineral assemblages in geologic systems. II. Equilibrium constraints in metamorphic/geothermal processes. *Am. J. Sci.* **281**, 576-614.

_____, SCHIFFMAN, P., ELDERS, W.A., WILLIAMS, A.E. & MCDOWELL, S.D. (1984): Calc–silicate mineralization in active geothermal systems. *Econ. Geol.* **79**, 671-695.

BISHOP, D.G. (1972): Progressive metamorphism from prehnite–pumpellyite to greenschist facies in the Dansey Pass area, Otago, New Zealand. *Geol. Soc. Am. Bull.* **83**, 3177-3198.

BROWNE, P.R.L. (1978): Hydrothermal alteration in active geothermal fields. *Ann. Rev. Earth Planet. Sci.* **6**, 229-250.

CAVARRETTA, G., GIANELLI, G. & PUXEDDU, M. (1982): Formation of authigenic minerals and their use as indicators of the physicochemical parameters of the fluid in the Larderello–Travale geothermal field. *Econ. Geol.* **77**, 1071-1084.

CHO, MOONSUP, LIOU, J.G. & MARUYAMA, S. (1986): Transition from the zeolite to prehnite–pumpellyite facies in the Karmutsen metabasites, Vancouver Island, British Columbia. *J. Petrol.* **27**, 467-494.

COLEMAN, R.G. (1977): *Ophiolite, Ancient Oceanic Lithosphere?* Springer–Verlag, New York.

COOMBS, D.S. (1960): Lower grade mineral facies in New Zealand. *21st Intern. Geol. Congr.*, **XIII**, 339-351.

_____, NAKAMURA, Y. & VUAGNAT, M. (1976): Pumpellyite–actinolite facies schists of the Taveyanne Formation near Loèche, Valais, Switzerland. *J. Petrol.* **17**, 440-471.

D'AMORE, F. & GIANELLI, G. (1984): Mineral assemblages and oxygen and sulphur fugacities in natural water–rock interaction processes. *Geochim. Cosmochim. Acta* **48**, 847-857.

_____ & PANICHI, C. (1980): Evaluation of deep temperatures of hydrothermal systems by a new gas geothermometer. *Geochim. Cosmochim. Acta* **44**, 549-556.

DE ROEVER, W.P. (1947): Igneous and metamorphic rocks in eastern central Celebes. *In* Geological Explorations in the Island of Celebes under the Leadership of H. A. Brouwer. North-Holland, Amsterdam (65-73).

ELDERS, W.A., HOAGLAND, J.R. & WILLIAMS, A.E. (1981): Distribution of hydrothermal mineral zones in the Cerro Prieto geothermal field of Baja California, Mexico. *Geothermics* **10**, 245-253.

EVARTS, R.C. & SCHIFFMAN, P. (1983): Submarine hydrothermal metamorphism of the Del Puerto ophiolite, California. *Am. J. Sci.* **283**, 289-340.

GIGGENBACH, W.F. (1980): Geothermal gas equilibria. *Geochim. Cosmochim. Acta* **44**, 2021-2032.

_____ (1981): Geothermal mineral equilibria. *Geochim. Cosmochim. Acta* **45**, 393-410.

HELGESON, H.C., DELANY, J.M., NESBITT, H.W. & BIRD, D.K. (1978): Summary and critique of the thermodynamic properties of rock-forming minerals. *Am. J. Sci.* **278-A**.

_____ & KIRKHAN, D.H. (1974): Theoretical prediction of the thermodynamic behavior of aqueous electrolytes at high pressures and temperatures. I. Summary of the thermodynamic/electrostatic properties of the solvent. *Am. J. Sci.* **274**, 1089-1198.

_____, _____ & FLOWERS, G.C. (1981): Theoretical prediction of the thermodynamic behavior of aqueous electrolytes at high pressures and temperatures. IV. Calculation of activity coefficients, osmotic coefficients, and apparent molal and standard and relative partial molal properties to 600°C and 5 kb. *Am. J. Sci.* **281**, 1249-1516.

HENLEY, R.W. & ELLIS, A.J. (1983): Geothermal systems ancient and modern: a geochemical review. *Earth-Sci. Rev.* **19**, 1-50.

HSU, L.C. (1968): Selected phase relationships in the system Al–Mn–Fe–Si–O–H: a model for garnet equilibria. *J. Petrol.* **9**, 40-83.

INOUE, A. & UTADA, M. (1989): Mineralogy and genesis of hydrothermal aluminous clays containing sudoite, tosudite, and rectorite in a drill hole near the Kamikita Kuroko ore deposit, northern Honshu, Japan. *Clay Sci.* **7**, 193-217.

LEE, M.S. (1970): Genesis of the lower ore bodies, Kaminosawa ore deposit, Kamikita mine, Aomori Prefecture, Japan. *Mining Geol.* **20**, 378-393 (in Japanese).

_____, MIYAZIMA, T. & MIZUMOTO, H. (1974): Geology of the Kamikita mine, Aomori Prefecture, with special reference to genesis of fragmental ores. *Mining Geol., Spec. Issue* **6**, 53-66.

LIOU, J.G. (1979): Zeolite facies metamorphism of basaltic rocks from the East Taiwan ophiolite. *Am. Mineral.* **64**, 1-14.

_____, MARUYAMA, S. & CHO MOONSUP (1987): Very low-grade metamorphism of volcanic and volcaniclastic rocks – mineral assemblages and mineral facies. *In* Low Temperature Metamorphism (M. Frey, ed.). Blackie, Glasgow (59-113).

MÉVEL, C. (1981): Occurrence of pumpellyite in hydrothermally altered basalts from the Vema Fracture Zone (Mid-Atlantic Ridge). *Contrib. Mineral. Petrol.* **76**, 386-393.

MIYAZIMA, T. & MIZUMOTO, H. (1965): Geology and ore deposits of the Kamikita mine, Aomori-ken. *Mining Geol.* **15**, 142-156 (in Japanese).

_____ & _____ (1968): Geology and ore deposits of the Kamikita mine, Aomori Prefecture (2), with special reference to the volcanism and mineralization in the Okunosawa Formation. *Mining Geol.* **18**, 185-199 (in Japanese).

NAKAJIMA, T., BANNO, S. & SUZUKI, T. (1977): Reactions leading to the disappearance of pumpellyite in low-grade metamorphic rocks of the Sanbagawa metamorphic belt in central Shikoku, Japan. *J. Petrol.* **18**, 263-284.

ROSE, N.M. & BIRD, D.K. (1987): Prehnite–epidote phase relations in the Nordre Aputiteq and Kruuse Fjord layered gabbros, East Greenland. *J. Petrol.* **28**, 1193-1218.

SCHIFFMAN, P., BIRD, D.K. & ELDERS, W.A. (1985):

Hydrothermal mineralogy of calcareous sandstones from the Colorado River delta in the Cerro Prieto geothermal system, Baja California, Mexico. *Mineral. Mag.* **49,** 435-449.

_____ & LIOU, J.G. (1980): Synthesis and stability relations of Mg–Al pumpellyite, $Ca_4Al_5MgSi_6O_{21}(OH)_7$. *J. Petrol.* **21,** 441-474.

_____ & _____ (1983): Synthesis of Fe-pumpellyite and its stability relations with epidote. *J. Metamorph. Geol.* **1,** 91-101.

SEKI, Y. (1973): Metamorphic facies of propylitic alteration. *J. Geol. Soc. Japan* **79,** 771-780.

SIGVALDASON, G.E. (1963): Epidote and related minerals in two deep geothermal drill holes, Reykjavik and Hveragerdi, Iceland. *U.S. Geol. Surv., Prof. Pap.* **450–E,** 77-79.

VIERECK, L.G., GRIFFIN, B.J., SCHMINCKE, H.-U. & PRITCHARD, R.G. (1982): Volcaniclastic rocks of the Reydarfjordur drill hole, eastern Iceland. 2. Alteration. *J. Geophys. Res.* **87B,** 6459-6476.

Received July 14, 1990, revised manuscript accepted November 30, 1990.